



# Comparing the capability of collision/reaction cell quadrupole and sector field inductively coupled plasma mass spectrometers for interference removal from $^{90}\text{Sr}$ , $^{137}\text{Cs}$ , and $^{226}\text{Ra}$

M.A. Amr\*, A.M. Abdel-Lateef

Central Laboratory for Elemental and Isotopic Analysis, Nuclear Physics Department, Atomic Energy Authority, Inshas, Cairo 13759, Egypt

## ARTICLE INFO

### Article history:

Received 27 August 2010

Received in revised form 30 October 2010

Accepted 1 November 2010

Available online 9 November 2010

### Keywords:

ICP-MS

Collision/reaction cell

$^{90}\text{Sr}$

$^{137}\text{Cs}$

$^{226}\text{Ra}$

## ABSTRACT

Here we report a quantitative comparison of sector field inductively coupled plasma mass spectrometry (ICP-SFMS) and collision/reaction cell inductively coupled plasma quadrupole mass spectrometry (ICP-QMS) for the detection of  $^{90}\text{Sr}$ ,  $^{137}\text{Cs}$ , and  $^{226}\text{Ra}$  at ultra-trace levels. We observed that the identification and quantification of radioisotopes by ICP-MS were hampered by spectral (both isobaric and polyatomic ions) and non-spectral (matrix effect) interferences. ICP-QMS has been used to eliminate the isobaric  $^{90}\text{Sr}/^{90}\text{Zr}$  interference through the addition of  $\text{O}_2$  into the collision cell as a reactant gas.  $\text{Zr}^+$  ions were subsequently converted into  $\text{ZrO}^+$ , whereas  $\text{Sr}^+$  ions were not reactive. In addition, the isobaric interference of  $^{137}\text{Ba}$  on  $^{137}\text{Cs}$  was eliminated by the addition of  $\text{N}_2\text{O}$  gas in the cell, which led to the formation of  $\text{BaO}^+$  and  $\text{BaOH}^+$  products, whereas  $\text{Cs}^+$  remained unreactive. Furthermore, He and  $\text{H}_2$  were used in the collision/reaction cell to eliminate polyatomic ions formed at  $m/z$  226. A comparison of the results obtained by ICP-SFMS after a chemical separation of Sr from Zr and Cs from Ba was performed. Finally, to validate the developed analytical procedures, measurements of the same samples were performed by  $\gamma$ -ray spectroscopy.

© 2010 Elsevier B.V. All rights reserved.

## 1. Introduction

Both natural and anthropogenic radionuclides are present in the environment. The major sources of natural radioactivity are the nuclides of very long half-lives, which have persisted since the formation of the earth [1]. Anthropogenic radionuclides can enter into the environment through a variety of different processes. The most relevant sources of artificial radioactivity are global fallout from atmospheric weapons tests, local fallout accidentally released from nuclear power plants, spent fuel reprocessing plants, and short-lived nuclides from the production of radioisotopes for different applications.

The most widely used analytical techniques for the determination of  $^{90}\text{Sr}$ ,  $^{137}\text{Cs}$ , and  $^{226}\text{Ra}$  are radioanalytical techniques [2].  $^{90}\text{Sr}$  is a pure  $\beta$ -emitter, so the radiometric methods, such as gas flow GM counting and liquid scintillation counting are normally used for direct measurement of  $^{90}\text{Sr}$  or alternatively via  $^{90}\text{Y}$  (also pure  $\beta$ -emitter), a short-lived ( $T_{1/2} = 2.67$  days) daughter of  $^{90}\text{Sr}$ . All these radiometric methods require previous chemical separation and pre-concentration in order to avoid interference from other radionuclides and problems with self-absorption due to the presence of calcium or stable strontium in the sample.  $^{137}\text{Cs}$ ,

a short-lived radionuclide (30.07 years), decays by emitting  $\beta$ -particles with maximum energies of 514 keV (94.4%) and 1175 keV (5.4%); it is accompanied by  $\gamma$ -ray emission of 661.7 keV (85.1%).  $^{137}\text{Cs}$  can thus be measured by  $\beta$ -counting and  $\gamma$ -spectrometry. The often common choice to use gamma-counting is a consequence of the high abundance of the 661.7 keV  $\gamma$ -ray from  $^{137}\text{Cs}$ . There is little self-adsorption in the sample due to high energy, a possibility of direct measurement, and a minimum of contamination during sample preparation.  $^{226}\text{Ra}$ , a long-lived radionuclide (1600 years), decays by emitting alpha particles with energies of 4.60 and 4.78 MeV to  $^{222}\text{Rn}$ , accompanied with an emission of 186.2 keV (3.59%)  $\gamma$ -ray.  $^{226}\text{Ra}$  can thus be determined by  $\alpha$ -spectrometry and  $\gamma$ -spectrometry. The  $\gamma$ -rays from its grand daughters  $^{214}\text{Bi}$  (609.3 keV (46.1%) and 1120.3 keV (15.1%)) and  $^{214}\text{Pb}$  (295.2 keV (19.3%) and 351.9 keV (37.6%)) can also be used for the determination of  $^{226}\text{Ra}$ . However, the major disadvantage of measurements of  $^{90}\text{Sr}$ ,  $^{137}\text{Cs}$ , and  $^{226}\text{Ra}$  by  $\gamma$ -spectrometry relates to the ingrowth time, which can take from days to several weeks depending on the sensitivity and precision required.

ICP-MS has become a preferred method for the rapid and accurate determination of some radioisotopes in several matrices due to its low sample consumption, high sensitivity, excellent precision, and multi-elemental analysis potential [3]. However, isobaric and polyatomic interferences can significantly affect the accuracy of ICP-MS analyses, especially for radioanalytes. The required mass resolution to separate the  $^{90}\text{Sr}/^{90}\text{Zr}$  and  $^{137}\text{Cs}/^{137}\text{Ba}$  interferences is

\* Corresponding author. Tel.: +20 974660834.

E-mail address: [amrewis@hotmail.com](mailto:amrewis@hotmail.com) (M.A. Amr).

**Table 1**  
Possible interferences on  $^{90}\text{Sr}$ ,  $^{137}\text{Cs}$ , and  $^{226}\text{Ra}$  from complex matrices.

$^{90}\text{Sr}$				$^{137}\text{Cs}$		$^{226}\text{Ra}$	
Species	Required resolution	Species	Required resolution	Species	Required resolution	Species	Required resolution
$^{90}\text{Zr}$	98,150	$^{16}\text{O}^{74}\text{Ge}$	8585	$^{137}\text{Ba}$	109,000	$^{88}\text{Sr}^{138}\text{Ba}^+$	1054
$^{50}\text{Ti}^{40}\text{Ar}$	57,706	$^{18}\text{O}^{72}\text{Ge}$	5755	$^{97}\text{Mo}^{40}\text{Ar}$	3500	$^{87}\text{Sr}^{139}\text{La}^+$	1076
$^{50}\text{V}^{40}\text{Ar}$	22,888	$^{16}\text{O}^{74}\text{Se}$	7639	$^{121}\text{Sb}^{166}\text{O}$	16,400	$^{86}\text{Sr}^{140}\text{Ce}^+$	1072
$^{50}\text{Cr}^{40}\text{Ar}$	31,961	$^{89}\text{Y}^1\text{H}$	10,748	$^{120}\text{Sn}^{17}\text{O}$	120,090	$^{186}\text{W}^{40}\text{Ar}^+$	2080
$^{52}\text{Cr}^{38}\text{Ar}$	37,855	$^{180}\text{Hf}^{++}$	1329	$^{136}\text{Xe}^1\text{H}$	17,200	$^{209}\text{Bi}^{16}\text{O}^1\text{H}^+$	5347
$^{53}\text{Cr}^{37}\text{Cl}$	95,950	$^{180}\text{Ta}^{++}$	1320	$^{136}\text{Ce}^1\text{H}$	17,300	$^{208}\text{Pb}^{18}\text{O}$	4556
$^{54}\text{Cr}^{36}\text{Ar}$	110,721	$^{180}\text{W}^{++}$	1327	$^{136}\text{Ba}^1\text{H}$	25,800		
$^{55}\text{Mn}^{35}\text{Cl}$	70,075	$^{45}\text{Sc}^{45}\text{Sc}$	14,496				
$^{54}\text{Fe}^{36}\text{Ar}$	58,342						

higher than 12,000, which is beyond the actual possibility of sector field mass spectrometers (e.g., JEOL, PlasmaX2).

Suppression of these interferences has been the subject of many investigations that have been reviewed elsewhere [4,5]. The reduction of polyatomic interferences can be accomplished using direct (instrumental) and indirect (sample preparation and treatment) techniques. ICP-SFMS, however, cannot resolve all of the interference problems, especially when a resolution higher than 10,000 is required to separate the analyte from the interference. This is the case for numerous interferences, such as  $^{90}\text{Zr}$  and  $^{89}\text{Y}^1\text{H}$  with  $^{90}\text{Sr}$ , and  $^{137}\text{Ba}$  and  $^{136}\text{Xe}^1\text{H}$  with  $^{137}\text{Cs}$ . Table 1 summarizes the isobaric and polyatomic interferences on  $^{90}\text{Sr}$ ,  $^{137}\text{Cs}$ , and  $^{226}\text{Ra}$ .

As an alternative to ICP-SFMS, ICP-QMS with collision/reaction cell has been proposed to reduce background noise and improve sensitivity for isotopic and trace analyses [6]. The collision–reaction cell was used to eliminate one or more interfering species (isobaric or polyatomic) that limit the analysis of some isotopes [6,7–16]. For this purpose, the gas injected into the cell must ideally react with the interference and have little to no reaction with the analyte of interest [17]. This reaction gas can be selected on the basis of thermodynamic and kinetic data. Based on studies of ion kinetics, dynamics, and thermochemistry, it is possible to use gas-phase reaction chemistry to overcome some polyatomic interferences without significant minimization in sensitivity [18].

Because ICP-SFMS and ICP-QMS are both powerful, yet complementary solutions toward the problem of detecting radioisotopes, a study that compares the two methods is necessary. Here we report a quantitative and qualitative evaluation of ICP-SFMS and ICP-QMS for the detection of  $^{90}\text{Sr}$ ,  $^{137}\text{Cs}$ , and  $^{226}\text{Ra}$  at ultra-trace levels. We also have developed and elucidated experimental details that aid in the minimization of isobaric and polyatomic interferences. Finally, we validated the findings presented here with  $\gamma$ -ray spectroscopy.

## 2. Experimental

### 2.1. Instrumentation

The measurements were performed on an ICP-QMS (Agilent, 7500Ce) that utilizes an octopole ion guide enclosed in a collision/reaction cell. A micromist nebulizer was fitted to a standard quartz double-pass spray chamber. The nebulizer was operated at  $2^\circ\text{C}$  to ensure temperature stability and to reduce the water vapor present in the carrier gas/aerosol stream. The samples (listed below) were driven into a standard quartz torch, which was fitted with the shield torch. Sector-field ICP-MS (JEOL, PlasmaX2) was used for comparison. A microconcentric nebulizer with a desolvation introduction system (Aridus, CETAC, Omaha, NE, USA) was used in the measurements. Argon (Ar), nitrous oxide ( $\text{N}_2\text{O}$ ), oxygen ( $\text{O}_2$ ), helium (He) and hydrogen ( $\text{H}_2$ ) gases used in the experiment were five-grade (99.999%). Table 2 summarizes the experimental conditions of the ICP-QMS and ICP-SFMS methods used in the measurements.

To evaluate the precision and accuracy of the proposed methods for measurements of the radionuclides by ICP-MS at ultra-trace levels, the samples were measured by  $\gamma$ -ray spectrometry. Gamma ray spectra were collected using a P-type coaxial EG&G Ortec HPGe detector with 25% relative efficiency and 1.9 keV FWHM at 1.33 MeV of  $^{60}\text{Co}$ . To measure  $^{137}\text{Cs}$  and  $^{226}\text{Ra}$ , the samples were counted after being quantitatively transferred into a Marinelli beaker and stored for progeny in-growth for one month. The samples were measured thereafter for a period of 1000 s.  $^{90}\text{Sr}$  was measured by  $\gamma$ -ray spectrometry after Mietelski and Męczyński [19]. Namely, the pottery samples in pellet form were sandwiched between two Cu discs of 1 mm thickness and 4 cm in diameter, and then the samples were put directly on the coaxial HpGe detector

**Table 2**  
Tuning parameters for the ICP-QMS (Agilent 7500Ce) and the ICP-SFMS (PlasmaX2).

ICP-QMS (Agilent 7500Ce)		ICP-SFMS (JEOL, PlasmaX2)	
Sample and skimmer cone	Nickel	Sample and skimmer cone	Copper
RF-power	850 W for Sr and Ra 800 W for Cs	RF-power	850 W for Sr and Ra 800 W for Cs
Sampling depth	8 mm	X, Y, Z torch position	Daily
Shielded torch	On	Shielded torch	On
Plasma gas flow rate	14.7 L/min	Cones accelerating voltage	6 kV
Auxiliary gas flow rate	0.8 L/min	Plasma gas flow rate	14 L/min
Makeup gas flow rate	0.2 L/min	Auxiliary gas flow rate	0.3 L/min
Nebulizer gas flow rate	0.8 L/min	Nebulizer gas flow rate	0.84 L/min
Peristaltic pump speed	0.1 rps	Spray chamber temperature	$4^\circ\text{C}$
Spray chamber temperature	$2^\circ\text{C}$	Switching	1000 ms
Extract lens 2	15 V	MF dwelling time	500 ms
Omega bias	–16 V	EF dwelling time	50 ms
Omega lens	2 V	Number of replicates	10
Cell entrance	–20 V		
Cell Exit	–15 V		
Quadruple potential	–12 V		

end-cap (sandwich counting geometry). The predetermined counting time for each measurement was 1000 s, and it was enough to obtain good counting statistics. Thus, the bremsstrahlung radiation energy spectra were obtained for the sandwich-counting geometries. The background spectra were also collected separately for sandwich geometries. Each bremsstrahlung radiation energy spectra was corrected for the background.

## 2.2. Standard and reagents

Multielement standard solutions of Sr, Zr, Cs, Sb, Sn, Ba, Mo, La, Ce, Pb, W, and Bi were obtained from AccuStandard, Inc., USA.  $^{226}\text{Ra}$  (SRM 4695),  $^{133}\text{Ba}$  (SRM 4251C),  $^{137}\text{Cs}$  (SRM 4233E), freshwater lake sediment standard reference material (SRM4354), and apple leaves standard reference material (NIST 1515) were purchased from the National Institute of Standards and Technology (NIST, Gaithersburg, MD, USA). In addition,  $^{130}\text{Ba}$  was purchased from Isoflex USA (San Francisco, CA, USA). All solutions were diluted with high-purity deionized water ( $18\text{ M}\Omega\text{ cm}^{-1}$ ) and then acidified with 2% ultrapure  $\text{HNO}_3$  (Merck, Germany). Three commercially available ionic resins, AG50W-X8, AG 1-X4 and Sr\*Spec were purchased from Eichrom Technologies (Darien, IL, USA).

Naturally-occurring radioactive materials (NORM) were taken from waste associated with oil and natural gas production in Abu-Rudeis, Egypt. The waste bulk contained mainly the sludge and scale formed inside the production equipment (e.g., pipelines, tank separators, and pumps). These wastes were removed periodically during the maintenance process.

## 2.3. Digestion of pottery and separation of strontium

Pottery samples were dried overnight at  $105^\circ\text{C}$  and ground to fine particles. About 0.5 g of each sample was weighed and transferred into a polytetrafluoroethylene (PTFE) beaker and moistened with a few milliliters of deionized water. Ten milliliters of HF and 4 mL of  $\text{HClO}_4$  were slowly added and evaporated on a hot plate at  $200^\circ\text{C}$  until a crystalline paste was formed (2–3 h). Four milliliters of  $\text{HClO}_4$  were added to each sample and evaporated to incipient dryness to remove any HF residue. Ten milliliters of 3-M  $\text{HNO}_3$  were added and warmed gently until a clear solution was obtained. Eichrom Sr-resin was conditioned with 10 mL of 8-M  $\text{HNO}_3$ . The samples were loaded (assuming retention of the Sr), and the resin was rinsed with 3 mL of 3-M  $\text{HNO}_3$ . Zirconium and other matrix elements were washed from the column to leave a pure Sr fraction on the column. Strontium was then eluted with 3 mL of distilled water.

## 2.4. Digestion of plants and separation of cesium

Approximately 0.5 g of sunflower (*Helianthus annuus* L.) was digested in a microwave digestion system (MarsX, CEM, Germany) using 7 mL of  $\text{HNO}_3$  and 2 mL of  $\text{H}_2\text{O}_2$ . Separation of Cs from Ba in the digested plants was performed using a method developed by Epov et al. [16]. Namely, 100 mL of a digested plant sample (1.5-M  $\text{HNO}_3$ ) was passed through a column containing 25 g of AG50W-X8 resin. The column was then rinsed with 10 mL of Milli-QPlus water. Cesium was eluted from the column using 4 mL of 5-M  $\text{HNO}_3$ . The final solution was analyzed by ICP-SFMS.

## 2.5. Pre-concentration of $^{226}\text{Ra}$ on $\text{MnO}_2$ impregnated resin

NORM samples were dried overnight at  $105^\circ\text{C}$  and ground to fine particles. Approximately 0.5 g of each sample was weighed and transferred into a PTFE beaker. Ten milliliters of HF and 4 mL of  $\text{HClO}_4$  were slowly added and evaporated on a hot plate at  $200^\circ\text{C}$  until a crystalline paste was formed. Then, 4 mL of  $\text{HClO}_4$  was added

to each sample and evaporated to incipient dryness to remove any HF residue. Finally, 10 mL of 0.05-M  $\text{HNO}_3$  was added and warmed gently until a clear solution was obtained.

Manganese dioxide-impregnated resin was prepared as reported by Varga [20]. Namely, 40 g of AG 1-X4 anion exchange resin (chloride form: 100–200 mesh) was placed in a 250-mL centrifuge tube with twice the volume of high-purity water and mixed thoroughly. Approximately 40 mL of saturated  $\text{KMnO}_4$  solution was added to the resin and mixed vigorously. After 15 min, the sample was centrifuged, and the supernatant was discarded. The resin was then rinsed three times with 80 mL of high-purity water, followed by centrifugation and discarding of the rinsing solution. The resin obtained was filtered gravimetrically through a Whatman filter and quantitatively transferred to a 250-mL plastic container with water. The resin was then dried at  $70^\circ\text{C}$  overnight. After drying, the resin was thoroughly homogenized with a plastic rod. The prepared  $\text{MnO}_2$  resin was transferred into a column for filtering, and the sample was loaded at a rate of  $1\text{ mL min}^{-1}$  [21]. The filter was then rinsed with ultrapure water and transferred into the 15-mL tubes for leaching with 1-M  $\text{HNO}_3$  in an ultrasonic bath for 1 h. The leached sample was filtered twice through a small Teflon filter and acidified with concentrated nitric acid to a molarity of approximately 3. Then, the sample (final volume  $\sim 15\text{ mL}$ ) was used for separation on the Eichrom “Sr-specific” resin because the  $\text{MnO}_2$  filter was selective for strontium [22].

## 3. Results and discussion

### 3.1. Determination of $^{90}\text{Sr}$ in pottery

#### 3.1.1. Measurements of $^{90}\text{Sr}$ using ICP-SFMS

A standard solution of Sr was used to optimize the instrument. The determination of  $^{90}\text{Sr}$  was hampered by isobaric interferences from  $^{90}\text{Zr}$ - and Ar-based ion species (Table 1). The resolution of  $^{90}\text{Zr}$  from  $^{90}\text{Sr}$  would therefore require a mass resolution of 98,150, which is beyond the capability of ICP-SFMS. Furthermore, the ionization energy of Sr was 5.70 eV, which is below the 1.14 eV ionization energy of Zr (6.84 eV) [23]. The radio frequency (rf) power was then reduced gradually from 1500 W to 800 W. Most of the elements have lower first ionization energies, so with cold plasma, reduced intensities of Ar-based ions and lower intensities of elements with high ionization energies, such as Zr, are expected [24].  $^{90}\text{Sr}$  was separated and pre-concentrated using Sr-resin, and then, measured under “cold” plasma conditions (800 W).

In order to minimize peak tailing on  $m/z=90$  the ICP-SFMS measurements were performed in the medium mass resolution mode ( $m/\Delta m=4000$ ). The abundance sensitivities for two mass-units above the tailing peak in ICP-SFMS were calculated using Eq. (1) [25]. The abundance sensitivity was found to be  $0.8 \times 10^{-7}$ , measuring  $500\ \mu\text{g mL}^{-1}$  of natural strontium.

$$\text{Abundance sensitivity} \left( \frac{m+2}{m} \right) = \frac{\text{intensity on}(m/z) = 90}{\text{intensity on}(m/z) = 88} \quad (1)$$

To increase the sensitivity in the cooled plasma condition, we inserted a plate between the torch and the RF coil. The shield plate eliminated the capacitive coupling between the plasma and the RF coil, which in turn eliminated the secondary discharge between the sampler and skimmer cones [26]. The production of a narrow ion energy distribution resulted in a higher transmission and, therefore, in an increase in sensitivity for analyte ions, such as Sr. Fig. 1 shows the observed enhancement in ion intensities of  $^{90}\text{Sr}$ ,  $^{137}\text{Cs}$ , and  $^{226}\text{Ra}$  using a shielded torch. The detection limit for  $^{90}\text{Sr}$  was calculated as the concentration equivalent to three times the standard deviation of the blank divided by the sensitivity [ $(\bar{X}_B + 3\sigma_B)/\text{sensitivity}$ , where  $\bar{X}_B$  is the mean of the background]. The detection limit was then calculated from the calibration curves

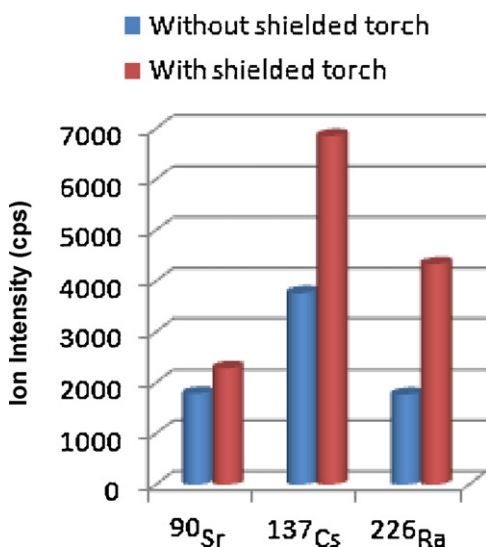


Fig. 1. Enhancement of ion intensities for 100 ppt  $^{90}\text{Sr}$ ,  $^{137}\text{Cs}$  and  $^{226}\text{Ra}$  using ICP-SFMS with a shielded torch.

for standard solutions of  $^{90}\text{Sr}$ . The detection limit was found to be 0.01 ppt using a microconcentric nebulizer with a desolvation introduction system (Aridus).

### 3.1.2. Separation of Sr/Zr isobars using $\text{O}_2$ in the ICP-QMS

Previously published work indicated that the reactive gases  $\text{CH}_3\text{F}$ ,  $\text{CH}_3\text{Cl}$ ,  $\text{SF}_6$ ,  $\text{NH}_3$ ,  $\text{D}_2\text{O}$ ,  $\text{CS}_2$ ,  $\text{CO}_2$ ,  $\text{N}_2\text{O}$  and  $\text{O}_2$  could be used to remove isobaric and polyatomic interferences from Sr isotopes [7–12]. The heat of reaction of  $\text{O}_2$  with the Sr, Zr and Y ions was calculated to be 47.8 kcal/mol, –88.7 kcal/mol, and –60.4 kcal/mol, respectively [9]; this indicates that the reaction with Sr is endothermic and not energetically favorable, whereas reactions with Zr and Y are exothermic and favored. Tanner et al. [17] pointed out that kinetic data must also be considered to make sure that an exothermic reaction does occur in the reaction cell (because of the small time of contact between the gas molecules and the ions). Data available from Koyanagi et al. [10] showed that the reaction of  $\text{O}_2$  with Zr and Y was efficient with yields of 82% and 67%, respectively, whereas no reaction between  $\text{Sr}^+$  and  $\text{O}$  was observed by the measuring technique [11]. Fig. 2 shows the profiles for the reaction of  $\text{Sr}^+$ ,  $\text{Zr}^+$  and  $\text{Y}^+$  ions with  $\text{O}_2$  measured by the ICP-QMS. The con-

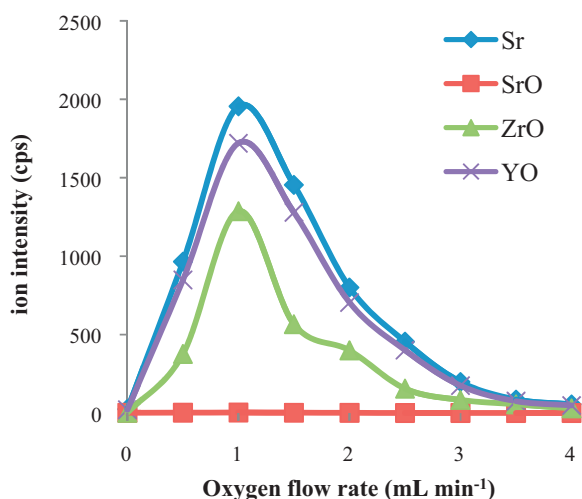


Fig. 2. Effect of  $\text{O}_2$  gas flow rate on the net signals of  $^{88}\text{Sr}$ ,  $^{89}\text{Y}$  and  $^{90}\text{Zr}$ . The concentrations of Sr, Zr and Y used were all 1 ppb.

Table 3  
Concentration of  $^{90}\text{Sr}$  (ppt) measured in pottery.

Time (h)	ICP-SFMS	ICP-QMS	$\gamma$ -Ray spectrometry
0.5	$0.54 \pm 0.05$	<DL	$3.14 \pm 0.2 \text{ Bq/g}$ ( $0.58 \pm 0.004$ )
1.0	$1.47 \pm 0.16$	$1.43 \pm 0.14$	$7.99 \pm 0.6 \text{ Bq/g}$ ( $1.46 \pm 0.011$ )
2.0	$3.35 \pm 0.15$	$3.45 \pm 0.11$	$18.3 \pm 0.6 \text{ Bq/g}$ ( $3.35 \pm 0.011$ )
3.0	$6.83 \pm 0.08$	$6.73 \pm 0.19$	$37.1 \pm 0.7 \text{ Bq/g}$ ( $6.79 \pm 0.013$ )
5.0	$8.74 \pm 0.15$	$8.84 \pm 0.14$	$47.5 \pm 1.1 \text{ Bq/g}$ ( $8.69 \pm 0.020$ )
7.0	$9.66 \pm 0.08$	$9.57 \pm 0.15$	$52.7 \pm 0.9 \text{ Bq/g}$ ( $9.65 \pm 0.016$ )
24.0	$9.79 \pm 0.09$	$9.89 \pm 0.14$	$54.5 \pm 1.8 \text{ Bq/g}$ ( $9.97 \pm 0.033$ )

centrations of Sr, Zr and Y used for this investigation were 1 ppb. At flow rates below  $1 \text{ mL min}^{-1}$ , the signals of  $^{89}\text{Y}^+$  and  $^{90}\text{Zr}^+$  decay relatively quickly, whereas the signal of  $^{88}\text{Sr}^+$  increases up to a maximum flow rate at  $1 \text{ mL min}^{-1}$ . The detection of  $^{90}\text{Sr}$  was successful at 0.92 ppt with a  $1 \text{ mL min}^{-1}$  flow rate of  $\text{O}_2$ .

### 3.1.3. Concentration of $^{90}\text{Sr}$ in pottery

The developed methods were next applied to measure the  $^{90}\text{Sr}$  adsorbed in pottery from aqueous solution. The capability of pottery pots to remove  $^{90}\text{Sr}$  from radioactive waste solution was investigated as low cost sorbents. To investigate this ability, 24 pottery containers (100 mL and thickness of 0.7 cm) were filled with a 0.1-ppt  $^{90}\text{Sr}$  standard solution. The pH of the solution was then adjusted to 7.5 using nitric acid and sodium hydroxide. The amount of  $^{90}\text{Sr}$  adsorbed into the pottery containers was analyzed by both mass spectrometry and  $\gamma$ -ray spectrometry (Table 3). The initial rapid removal that was followed by a slower removal of  $^{90}\text{Sr}$  by the pottery suggested two sorption processes: ion exchange and adsorption in the beginning, followed by a slow penetration of metal ions into the crystal lattice of the minerals forming the pottery. Because pottery constituents are principally  $\text{SiO}_2$ ,  $\text{Al}_2\text{O}_3$  and  $\text{Fe}_2\text{O}_3$ , the existence of various adsorption/exchange sites is highly probable. Therefore, the mechanisms of metal ion removal may include physical and chemical adsorption and/or ion exchange. The resulting precisions (RSD) of the measurements were in the range of 2.13–7.42%. The poor precision was due to the low ion intensity of  $^{90}\text{Sr}$  in the pot samples.

## 3.2. Determination of $^{137}\text{Cs}$ in sunflower (*H. annuus L.*)

### 3.2.1. Measurements of $^{137}\text{Cs}$ using ICP-SFMS

The determination of  $^{137}\text{Cs}$  was hampered by an isobaric interference from  $^{137}\text{Ba}$  and other polyatomic ions shown in Table 1. The resolution of  $^{137}\text{Ba}$  from  $^{137}\text{Cs}$  would, therefore, require a mass resolution of 109,000, which is beyond the capability of ICP-SFMS. A standard solution of Cs, Ba, Sb, Sn, and Mo was measured under different plasma powers as shown in Fig. 3. At low plasma power (800 W), the polyatomic ion species were reduced. By decreasing the plasma power to 750 W, the ion intensity of Ba was reduced to ~5 counts per second (cps). Although the ion intensity of Cs at 800 W was maximal, traces of  $^{137}\text{Ba}$  still ionized and interfered with  $^{137}\text{Cs}$ . These results indicated that a chromatographic separation of Cs from Ba was necessary to measure  $^{137}\text{Cs}$  at ultra-trace levels by ICP-SFMS. Concentrations of 0.5, 1, and 10 ppt of  $^{137}\text{Cs}$  were used to calibrate the instrument. The detection limit was calculated from the calibration curve of  $^{137}\text{Cs}$  and found to be 0.045 ppt using a microconcentric nebulizer with a desolvation introduction system (Aridus).

### 3.2.2. Cs/Ba separation by ICP-QMS

Three recent studies have illustrated that the Cs–Ba isobaric interference could be suppressed by  $\text{H}_2$  and He mixtures,  $\text{N}_2\text{O}$ , and  $\text{CH}_3\text{Cl}$  [6,13–15]. However,  $\text{H}_2$  and He efficiencies were found to require optimized conditions after separation and preconcentration for more than 0.5 ppb of Ba [6].

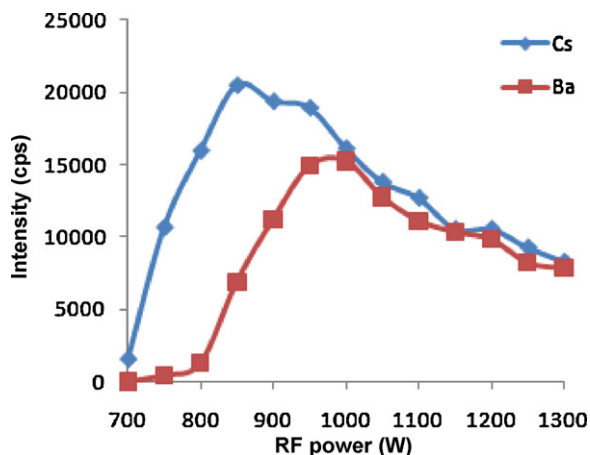


Fig. 3. Effect of RF power on the response of  $^{133}\text{Cs}$  and  $^{137}\text{Ba}$  with ICP-SFMS. Cs and Ba concentrations were 1 ppb.

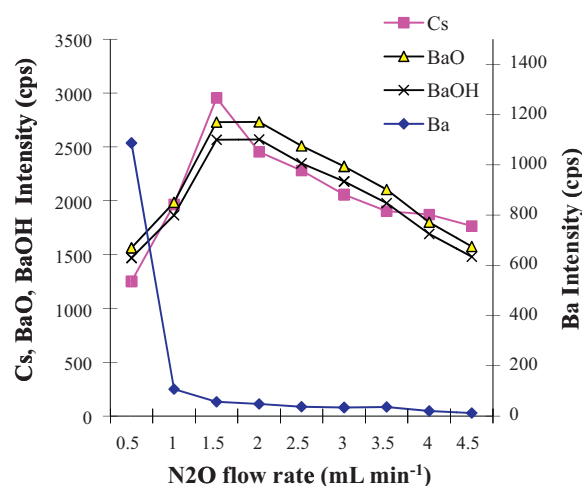


Fig. 4. Effect of  $\text{N}_2\text{O}$  gas flow rate on the signal intensities of  $^{133}\text{Cs}^+$ ,  $^{137}\text{Ba}$ ,  $^{138}\text{Ba}^{16}\text{O}$ , and  $^{138}\text{Ba}^{16}\text{O}^1\text{H}$ . The concentrations of Cs and Ba were 10 ppb.

For  $\text{N}_2\text{O}$ , the available thermodynamic data [27] indicated that only Ba should be reactive to this gas. The heat of reaction of  $\text{N}_2\text{O}$  with  $\text{Cs}^+$  to form  $\text{CsO}^+$  is 106.3 kJ/mol and is endothermic, so the reaction is not likely to occur. However, the heat of reaction of  $\text{Ba}^+$  with  $\text{N}_2\text{O}$  to form  $\text{BaO}^+$  is  $-236.8$  kJ/mol, making it exothermic and thermodynamically favored.

As thermodynamic data only give indications of the feasibility of the reactions, kinetic aspects must also be considered to investigate reaction efficiencies. A standard solution of Cs and Ba at concentrations of 10 ppb was aspirated through an octopole reaction cell ICP-QMS. The effect of  $\text{N}_2\text{O}$  on the resulting ion intensities of Cs and Ba are shown in Fig. 4. The  $^{133}\text{Cs}$  signal increased for  $\text{N}_2\text{O}$  flow rates up to  $1.5\text{ mL min}^{-1}$ . No reaction products were observed for Cs with  $\text{N}_2\text{O}$  in the cell. In contrast, the Ba signal, registered at mass 137, decreased rapidly and became negligible at a  $1.5\text{ mL min}^{-1}$   $\text{N}_2\text{O}$  flow rate, while a maximum intensity was observed at mass 154, highlighting the formation of  $^{138}\text{Ba}^{16}\text{O}$ . Additionally, a maximum intensity was reached at mass 155 for a higher gas flow rate

( $2\text{ mL min}^{-1}$ ), which accounts for the asynchronous formation of  $^{138}\text{Ba}^{16}\text{O}^1\text{H}$  compared to  $\text{BaO}$ .

The reactions of Sb and Sn (100-ppb natural solutions) towards  $\text{N}_2\text{O}$  gas have also been investigated and led to the formation of SbO and SnO species with an oxide formation rate of about 0.1% for both elements at a  $\text{N}_2\text{O}$  flow rate equal to  $1.5\text{ mL min}^{-1}$ . Very low yields of SbO and SnO were expected because of the very low ionizations of Sb and Sn at an RF power of 800 W (ionization energies of Sb and Sn are 8.641 eV and 7.344 eV, respectively) [23].

### 3.2.3. Concentration of $^{137}\text{Cs}$ in sunflower (*H. annuus L.*)

From the literature, one could gather that the sunflower (*H. annuus L.*) is a promising candidate for phytoremediation [28]. This effect has been studied in hydroponics trials on a laboratory scale and on a field scale for the decontamination of soils and water containing low to moderate levels of heavy metals, artificial radionuclides, and natural radionuclides [29]. In some cases, *H. annuus* contained 1000 times more metal than the soil in which it grew [30].

Twenty sunflower seedlings (*H. annuus L.*) were grown hydroponically in 1 L of water containing a nutrient solution for 4 weeks. The nutrient solution was prepared with (in g/L) 0.708  $\text{Ca}(\text{NO}_3)_2 \cdot 4\text{H}_2\text{O}$ , 0.492  $\text{MgSO}_4 \cdot 7\text{H}_2\text{O}$ , 0.17  $\text{KNO}_3$ , 0.272  $\text{KH}_2\text{PO}_4$ , 0.0083  $\text{FeCl}_3$ , 0.0025  $\text{H}_3\text{BO}_3$ , 0.0015  $\text{MnCl}_2 \cdot 4\text{H}_2\text{O}$ , 0.0001  $\text{ZnCl}_2$ , 0.00005  $\text{CuCl}_2 \cdot 2\text{H}_2\text{O}$ , 0.00005  $\text{Na}_2\text{MoO}_4 \cdot 2\text{H}_2\text{O}$ , and 0.0042 of other microelements [29]. Then, 0.1 ppt of  $^{137}\text{Cs}$  was added to the solution after 4 weeks. The plants were harvested 1 week after this addition. The harvested plants were divided by cutting into shoots and roots. After washing with de-ionized water, the plant tissues were dried at  $70^\circ\text{C}$  for 24 h and weighed. First, the active concentration of  $^{137}\text{Cs}$  was measured by  $\gamma$ -ray spectrometry in shoots and roots. Second, the shoots and roots were digested in a microwave digestion system. Chromatographic separation was then applied to separate  $^{137}\text{Cs}$  for measurements by ICP-SFMS. Another aliquot of digested shoots and/or roots was measured directly by ICP-QMS. The results are shown in Table 4.

### 3.3. Determination of $^{226}\text{Ra}$ in NORM

#### 3.3.1. Measurements of $^{226}\text{Ra}$ using ICP-SFMS

The possible formation of polyatomic interferences between inert gases (other than Ar), present as impurities in the plasma (Xe and Kr), and some transition (Mo) and lanthanide elements (Ce and Nd) was studied. At concentrations of  $1\ \mu\text{g mL}^{-1}$ , no change in the background signal at  $m/z=226$  was detected. Therefore, the formation of  $^{92}\text{Mo}^{134}\text{Xe}$ ,  $^{94}\text{Mo}^{132}\text{Xe}$ ,  $^{95}\text{Mo}^{131}\text{Xe}$ ,  $^{96}\text{Mo}^{130}\text{Xe}$ ,  $^{97}\text{Mo}^{129}\text{Xe}$ ,  $^{98}\text{Mo}^{128}\text{Xe}$ ,  $^{100}\text{Mo}^{126}\text{Xe}$ ,  $^{140}\text{Ce}^{86}\text{Kr}$ ,  $^{143}\text{Nd}^{83}\text{Kr}$ ,  $^{144}\text{Nd}^{82}\text{Kr}$ ,  $^{146}\text{Nd}^{80}\text{Kr}$ ,  $^{148}\text{Nd}^{78}\text{Kr}$  and  $^{146}\text{Nd}^{40}\text{Ar}^{40}\text{Ar}$  was not detected. A background equivalent concentration (BEC) was measured when  $1\ \mu\text{g mL}^{-1}$  of single solutions composed of W, Bi, Pb, Sr/La, Sr/Ce, and Sr/Ba were aspirated, as shown in Table 5. The results were found to be in agreement with data previously published [6,22,31]. Based on these data, a separation of radium was required.

#### 3.3.2. Polyatomic removal at $m/z$ 226 using ICP-QMS

The instrument was first optimized for a maximum ion intensity with a 10 ppt standard solution of  $^{226}\text{Ra}$ . Flow rates of helium and hydrogen, the octapole exit, and the octapole bias in the collision

Table 4  
Concentration of  $^{137}\text{Cs}$  (ppt) measured in sunflower (*Helianthus annuus L.*).

$^{137}\text{Cs}$ added	Species	ICP-SFMS	ICP-QMS	$\gamma$ -Ray spectrometry
0.1 ppt	Root	$36.3 \pm 1.9$	$35.8 \pm 1.4$	$123 \pm 3.8\text{ Bq/g}$ ( $36.6 \pm 1.1$ )
	Shoot	$24.2 \pm 1.5$	$23.4 \pm 1.7$	$79 \pm 4.2\text{ Bq/g}$ ( $23.5 \pm 1.2$ )

**Table 5**

Background equivalent concentrations (BEC) generated by aspiration of 1- $\mu\text{g mL}^{-1}$  solutions of W, Bi, Pb, Sr/La, Sr/Ce, and Sr/Ba.

Polyatomic ions	BEC (fg mL <sup>-1</sup> )
<sup>88</sup> Sr <sup>138</sup> Ba <sup>+</sup>	4.8
<sup>87</sup> Sr <sup>139</sup> La <sup>+</sup>	3.8
<sup>86</sup> Sr <sup>140</sup> Ce <sup>+</sup>	4.3
<sup>186</sup> W <sup>140</sup> Ar <sup>+</sup>	42
<sup>209</sup> Bi <sup>16</sup> O <sup>1</sup> H <sup>+</sup>	76
<sup>208</sup> Pb <sup>18</sup> O	10.2

cell were then optimized. After optimization of all the instrumental conditions, a multielement standard solution composed of W, Bi, Pb, Sr, La, Ce, and Ba was aspirated as a blank to estimate the background at  $m/z = 226$ . Another aliquot of the same solution was spiked with 10 ppt of <sup>226</sup>Ra and aspirated as a standard. In addition, the flow rates of He and H<sub>2</sub> in the collision cell were varied between 0 and 5 mL min<sup>-1</sup> to obtain the highest S/N for <sup>226</sup>Ra. Pressurizing the collision cell with He gas led to collision with the polyatomic and elemental ions. Since collisions with the larger cross-section polyatomic ions occurred more frequently than those with the elemental ions, polyatomic ion energy selectively decreased (Fig. 5). The application of an energy difference potential between the octopole (−15 V) and quadrupole (−12 V) prevented the lower energy polyatomic ions from entering the quadrupole and allowing the passage of the elemental ions under investigation. The detection limit was then calculated from the calibration curve using standard solutions of <sup>226</sup>Ra (5, 10, and 20 ppt). Furthermore, the detection limit of <sup>226</sup>Ra was found to be 0.31 ppt.

### 3.3.3. Radium-226 concentrations in NORM samples

NORM samples were dried overnight at 105 °C and then ground to a fine powder. One gram of NORM was weighed and transferred into a PTFE beaker. A total of 10 mL of HF and 4 mL of HClO<sub>4</sub> were slowly added and evaporated on a hot plated at 200 °C until a crystalline paste was formed (2–3 h). Four milliliters of HClO<sub>4</sub> was added to each sample and evaporated to incipient dryness to remove any HF residue. A total of 10 mL of 5-M HNO<sub>3</sub> was added and warmed gently until a clear solution was obtained. The clear solutions were allowed to cool and then diluted to 1000 mL in polypropylene bottles producing a 0.05-M HNO<sub>3</sub> solution. To estimate radium recovery, the solutions were spiked with 10 pg mL<sup>-1</sup>

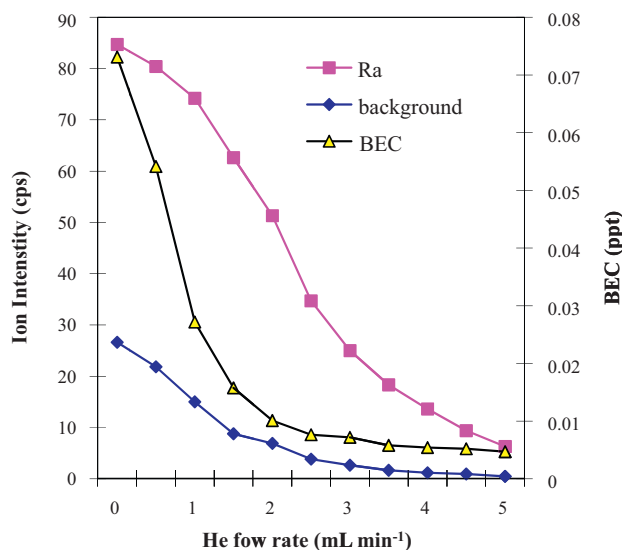


**Fig. 5.** BEC and reduction of count rates at  $m/z$  226 with increasing He gas flow at 1 mL min<sup>-1</sup> of H<sub>2</sub>.

**Table 6**

Concentrations of <sup>226</sup>Ra (ppt) in NORM measured by ICP-MS and  $\gamma$ -ray spectrometry.

Samples	ICP-SFMS	ICP-QMS	$\gamma$ -Ray spectrometry
NORM1	3.43 $\pm$ 0.08	3.46 $\pm$ 0.14	129 $\pm$ 5.6 Bq kg <sup>-1</sup> (3.52 $\pm$ 0.15)
NORM2	2.76 $\pm$ 0.14	2.69 $\pm$ 0.18	97 $\pm$ 3.2 Bq kg <sup>-1</sup> (2.65 $\pm$ 0.09)
NORM3	2.91 $\pm$ 0.12	2.92 $\pm$ 0.18	102 $\pm$ 6.8 Bq kg <sup>-1</sup> (2.97 $\pm$ 0.19)

of <sup>130</sup>Ba. The concentrations of <sup>226</sup>Ra in the samples were then measured using ICP-MS after pre-concentration and separation from strontium. Furthermore, 250 g from each NORM was collected and dried overnight. The NORM was then transferred into a Marinelli beaker and locked for progeny in-growth for one month. The resulting measured concentrations of <sup>226</sup>Ra by ICP-MS were within  $\pm 2\%$  of the measured concentrations of <sup>226</sup>Ra found by  $\gamma$ -ray spectrometry. The results of these experiments are shown in Table 6. For comparison, US-EPA regulations suggest that the maximum concentration of radium in soils is 1.38 pg g<sup>-1</sup> (50 Bq kg<sup>-1</sup>) [32].

## 4. Conclusion

This study showed that an ICP-MS with a collision/reaction cell offered an efficient way to directly eliminate the isobaric interference between <sup>90</sup>Sr and <sup>90</sup>Zr with oxygen addition. In addition, N<sub>2</sub>O addition caused Ba<sup>+</sup> to react, leading to the formation of BaO<sup>+</sup> and BaOH<sup>+</sup>, whereas Cs<sup>+</sup> remained unreactive due to its inability to form bonds. These analytical methods provided a means to directly measure the concentration of <sup>90</sup>Sr or <sup>137</sup>Cs in a sample with high precision and accuracy and without chemical separation from the matrix.

Extraction chromatography followed by measurements with ICP-SFMS at cooled plasma conditions was shown to eliminate possible isobaric and/or polyatomic interferences with <sup>90</sup>Sr, <sup>137</sup>Cs, or <sup>226</sup>Ra.

The time required for the measurement of <sup>90</sup>Sr, <sup>137</sup>Cs, or <sup>226</sup>Ra by ICP-SFMS was 2 days, which is significantly shorter than any radioanalytical protocol currently available. Overall, the determination of <sup>90</sup>Sr, <sup>137</sup>Cs, or <sup>226</sup>Ra could be performed within 1 day by ICP-QMS.

## References

- [1] A.I. Helal, N.F. Zahran, M.A. Amr, A.M. Abdel El-Lateef, I.I. Baster, H.T. Mohsen, Y. Abbas, *Radiochem. Acta* 92 (2004) 369–374.
- [2] X. Hou, P. Roos, *Anal. Chim. Acta* 608 (2008) 105–139.
- [3] J.S. Becker, *Int. J. Mass Spectrom.* 242 (2005) 183–195.
- [4] D.R. Bandura, V.I. Baranov, S.D. Tanner, *Fresen. J. Anal. Chem.* 370 (2001) 454–470.
- [5] M.R. Cave, O. Butler, S.R.N. Chenery, J.M. Cook, M.S. Cresser, D.L. Miles, *J. Anal. Atom. Spectrom.* 16 (2001) 194–235.
- [6] V.N. Epov, V. Taylor, D. Lariviere, R.D. Evans, R.J. Cornett, *J. Radioanal. Nucl. Chem.* 258 (2003) 473–482.
- [7] A.P. Vonderheide, M.V. Zoriy, A.V. Izmer, C. Pickhardt, J.A. Caruso, P. Ostapczuk, R. Hille, J.S. Becker, *J. Anal. Atom. Spectrom.* 19 (2004) 675–680.
- [8] G. Favre, R. Brennetot, F. Chartier, P. Vitorge, *Int. J. Mass Spectrom.* 265 (2007) 15–22.
- [9] H. Isnard, M. Aubert, P. Blanchet, R. Brennetot, F. Chartier, V. Geertsen, F. Manuguerra, *Spectrochim. Acta B* 61 (2006) 150–156.
- [10] G.K. Koyanagi, D. Caraiman, V. Blagojevic, D.K. Bohme, *J. Phys. Chem. A* 106 (2002) 4581–4590.
- [11] L.A. Simpson, R. Hearn, S. Merson, T. Catterick, *Talanta* 65 (2005) 900–906.
- [12] P. Cheng, G.K. Koyanagi, D.K. Bohme, *Anal. Chim. Acta* 627 (2008) 148–153.
- [13] J. Darrouzés, M. Bueno, G. Lespés, M. Holeman, M. Potin-Gautier, *Talanta* 71 (2007) 2080–2084.
- [14] V. Lavrov, V. Blagojevic, G. Koyanagi, G. Orlova, D. Bohme, *J. Phys. Chem. A* 108 (2004) 5610–5624.
- [15] M.A. Amr, K.A. Al-Saad, A.I. Helal, *Nucl. Instrum. Meth. A* 615 (2010) 237–241.
- [16] V.N. Epov, D. Lariviere, K.M. Reiber, R.D. Evans, R.J. Cornetta, *J. Anal. Atom. Spectrom.* 19 (2004) 1225–1229.
- [17] S.D. Tanner, V.I. Baranov, D.R. Bandura, *Spectrochim. Acta B* 57 (2002) 1361–1452.
- [18] D.R. Bandura, V.I. Baranov, A.E. Litherland, S.D. Tanner, *Int. J. Mass Spectrom.* 256 (2006) 312–327.

- [19] J.W. Mietelski, W. Męczyński, *Appl. Radiat. Isotopes* 53 (2000) 121–126.
- [20] Z. Varga, *Appl. Radiat. Isotopes* 65 (2007) 1095–1100.
- [21] M.V. Zoriy, Z. Varga, C. Pickhardt, P. Ostapczuk, R. Hille, L. Halicz, I. Segald, J.S. Becker, *J. Environ. Monit.* 7 (2005) 514–518.
- [22] D. Larivière, D.K. Brownell, V.N. Epov, R.J. Cornett, R.D. Evans, *J. Radioanal. Nucl. Chem.* 273 (2007) 337–344.
- [23] S.G. Lias, J.E. Bartmess, J.F. Liebman, J.L. Holmes, R.D. Levin, W.G. Mallard, *J. Phys. Chem. Ref. Data* 17 (Suppl. 1) (1988) 1–861.
- [24] M.V. Zoriy, P. Ostapczuk, L. Halicz, R. Hille, J.S. Becker, *Int. J. Mass Spectrom.* 242 (2005) 203–209.
- [25] M.V. Zoriy, L. Halicz, M.E. Ketterer, C. Pickhardt, P. Ostapczuk, J.S. Becker, *J. Anal. Atom. Spectrom.* 19 (2004) 362–367.
- [26] K.A. Al-Saad, M.A. Amr, A.I. Helal, *Biol. Trace Elem. Res.*, doi:10.1007/s12011-010-r-8677-2, in press.
- [27] M. Granet, A. Nonell, G. Favre, F. Chartier, H. Isnard, J. Moureau, C. Caussignac, B. Tran, *Spectrochim. Acta B* 63 (2008) 1309–1314.
- [28] E. Meers, A. Ruttens, M.J. Hopgood, D. Samson, F.M.G. Tack, *Chemosphere* 58 (2005) 1011–1022.
- [29] F. Vera Tomé, P. Blanco Rodríguez, J.C. Lozano, *Sci. Total Environ.* 393 (2008) 351–357.
- [30] M.F. AbdEl-Sabour, *EJEAFChE* 6 (2007) 2009–2023.
- [31] C.J. Park, P.J. Oh, H.Y. Kim, D.S. Lee, *J. Anal. Atom. Spectrom.* 14 (1999) 223–227.
- [32] Agency for Toxic Substances and Disease Registry, *Toxicology Profile for Radium*, U.S. Department of Health and Human Services, Washington, DC, 1990.